

# Deep convolution neural network for screening carotid calcification in dental panoramic radiographs

Moshe Amitay<sup>1,2</sup>, Zohar Barnett-Itzhaki<sup>1,3,4,\*</sup>, Shiran Sudri<sup>5</sup>, Chana Drori<sup>1</sup>, Tamar Wase<sup>1</sup>, Imad Abu-El-Naaj<sup>5,6</sup>, Merton Rieck<sup>1</sup>, Yossi Avni<sup>1</sup>, Gil Pogozelech<sup>1</sup>, Ervin Weiss<sup>1,7</sup> and Morris Mosseri<sup>1,8</sup>

<sup>1</sup> ODMachine, Herzlyia, Israel

<sup>2</sup> Bioinformatic Department, Jerusalem College of Technology, Jerusalem 9372115, Israel

<sup>3</sup> Faculty of Engineering, Ruppin Academic Center, Emek Hefer, Israel.

<sup>4</sup> Ruppin Research Group in Environmental and Social Sustainability, Ruppin Academic Center, Israel

<sup>5</sup> Department of Oral and Maxillofacial Surgery, Baruch Padeh Medical Center, Poriya, affiliated with Azrieli Faculty of medicine, Bar Ilan University, Israel.

<sup>6</sup> Azrieli Faculty of Medicine, Bar Ilan University, Safed, Israel

<sup>7</sup> Goldschleger School of Dental Medicine, Sackler Faculty of Medicine, Tel Aviv University, Tel Aviv, Israel

<sup>8</sup> Sackler Faculty of Medicine, Tel Aviv University

\*Corresponding author

E-mail: [zohar@od-machine.com](mailto:zohar@od-machine.com)

## 1 Abstract

- 2 Ischemic stroke, a leading global cause of death and disability, is caused by carotid arteries
- 3 atherosclerosis. Such calcifications are classically detected by ultrasound screening. In recent years it

4 was shown that these calcifications can also be inferred from routine panoramic dental radiographs.  
5 In this work, we focused on the panoramic dental radiographs taken from 500 patients, manually  
6 labelling each of the patients' sides (each radiograph was treated as two sides), and which were used  
7 to develop an artificial intelligence (AI)-based algorithm to automatically detect carotid  
8 calcifications. The algorithm uses deep learning convolutional neural networks (CNN), with transfer  
9 learning (TL) approaches followed by eXtreme Gradient Boosting algorithm (XGBoost) that achieved  
10 true labels for each corner, and reaches a sensitivity (recall) of 0.82 and a specificity of 0.93 for  
11 individual artery, and a recall of 0.88 and specificity of 0.86 for individual patients. Applying and  
12 integrating the algorithm we developed in healthcare units and dental clinics has the potential of  
13 reducing stroke events and their mortality and morbidity consequences.

#### 14 **Author summary**

15 Stroke is a leading global cause of death and disability. One major cause of stroke is carotid artery  
16 calcification (CAC). Traditional approaches for CAC detection are doppler ultrasound screening and  
17 angiography computerized tomography (CT), medical procedures that require financial expenses, are  
18 time consuming and discomforting to the patient. Of note, angiography CT involves the injection of  
19 contrast material and exposure to x-ray ionizing irradiation. In recent years researchers have shown  
20 that CAC can also be detected when analyzing routine panoramic dental radiographs, a non-  
21 invasive, cheap and easily accessible procedure. This study takes us one step further, in developing  
22 artificial intelligence (AI)-based algorithms trained to detect such calcifications in panoramic dental  
23 radiographs. The models developed are based on deep learning convolutional neural networks,  
24 transfer learning, and XGBoost algorithm, that enable an accurate automated detection of carotid  
25 calcifications, with a recall of 0.82 and a specificity of 0.93. Statistical approaches for assessing  
26 predictions per individual (*i.e.*: predicting the risk of calcification in at least one artery), were  
27 developed showing a recall of 0.88 and specificity of 0.86. Applying and integrating this approach in  
28 healthcare units may significantly contribute to identifying at-risk patients.

## 29 **Introduction**

30 Stroke is the third leading cause of death and the leading cause of disability in the Western world.  
31 Ischemic stroke is caused by carotid arteries atherosclerosis, small intracranial vessel disease or  
32 emboli from the heart and aorta [1,2]. The lifelong risk of stroke in adult men and women (age 25  
33 and older) is about 25 percent [3]. Ten percent of strokes are caused by intracerebral hemorrhage  
34 and 87% of all strokes are ischemic [2]. Several studies showed that patients aged 60-96 with carotid  
35 artery calcification (CAC) found in panoramic radiograph are 2.4 fold more likely to suffer from  
36 vascular events, including stroke and/or ischemic heart diseases [4,5].

37 Standard tests for detecting CAC are doppler ultrasound (US) and angiography computerized  
38 tomography (CT). However, there is evidence that calcification can be detected in panoramic dental  
39 X-rays (dental radiographs). These X-rays are routinely performed in daily practice by dentists and  
40 oral and maxillofacial surgeons [6]. A panoramic radiograph is a two-dimensional interpretation of  
41 tomographic images of curved anatomic structures. Panoramic radiography images serve as a  
42 diagnostic tool, and the image encompasses the teeth, the maxillary and mandibular bones,  
43 temporomandibular joints, and the maxillary sinus. Nonetheless, most dental professionals, dentists  
44 as well as specialists, are not trained for detecting and diagnosing CAC in panoramic X rays. Several  
45 studies focused on evaluating the ability of panoramic radiographs to detect CAC [5]. Recent meta-  
46 analyses of these studies revealed that the level of agreement between panoramic radiography and  
47 the above standard methods is 50% [7]. However, even with this limitation, panoramic radiography  
48 is more prevalent by far than US or coronary angiography (CAG). CAG is more available, but its use as  
49 a diagnostic tool is mostly overlooked. Therefore, panoramic radiography may play an important  
50 role in the screenig and detection of non-symptomatic CAC patients in the population.

51 Deep neural networks are a branch of machine learning (ML) and artificial intelligence (AI). These  
52 networks were developed to tackle complex challenges such as speech recognition, natural language  
53 processing, and also image classification and object recognition [8]. Deep learning architectures and

54 algorithms use multilayer artificial neural network (NN) architecture, a major class of deep learning  
55 algorithms is the convolutional neural networks (CNN), that are widely used for image classification  
56 [9].

57 Major challenges in the development of an efficient CNN classifier are the requirement for large  
58 numbers of training samples (usually >1,000 for each class), in addition to the long and  
59 comprehensive process of training a model. In order to cope with these challenges, transfer learning  
60 (TL) approach was developed. In this approach, the CNN training is not created from scratch, but  
61 partially uses an existing pre-trained model as a starting point [10,11]. The pre-trained model was  
62 previously trained on a different task using large amounts of data.

63 CNN and TL have been widely used in the prediction of medical conditions using different techniques  
64 (CT, MRI, panoramic images) - for example: identification of prostate cancer [12]; prediction of  
65 bladder cancer treatment response in CT [13]; detection of maxillary sinusitis on panoramic  
66 radiographs [14]; screening for osteoporosis in dental panoramic radiographs [15]; cardiac cine  
67 segmentation [16] and even COVID-19 detection from chest CT-scans [17].

68 In this study we aimed to develop and evaluate an image classifier for screening carotid calcification  
69 (CAC) in standard dental panoramic radiograph (DPR) images.

70 We trained and tested a convolutional neural network (CNN) followed by eXtreme Gradient Boosting  
71 algorithm (XGBoost) for CAC detection of a single carotid (one side of the image) and then calculated  
72 the performance of a full panoramic radiography images.

73

## 74 **Results**

75 500 patients participated in the cohort. The average age was 67.5, with a range of  $\pm 13.3$  years, 56%  
76 were male and 44% were female. 19.7% of the patients are smokers, 40% had diabetes, 63.7% had  
77 hypertension and 41.6% had history of cardiac infarction

78 Table 1 presents the prediction performance blind tests and shows that the classifier succeeded to  
79 find 82% of the CAC images. The prevalence of the real CACs in the predicted positives was 71%.

80 The Recall-Precision (RP) curve for all the cross-validation folds is presented in Figure 1. A RP curve is  
81 more informative than the usual ROC curve when the test is imbalanced and the performance on the  
82 minority class (*i.e* the CAC) is more important. The curves show the trade-off between recall and  
83 precision of the seven folds. It can be noticed that fold 3 slightly deviated from the rest of the folds.  
84 Thus, the actual performance may be somewhat better than the above. In addition, these curves  
85 show that we can achieve a higher recall value of 90% at the cost of decreasing the precision to 60%.

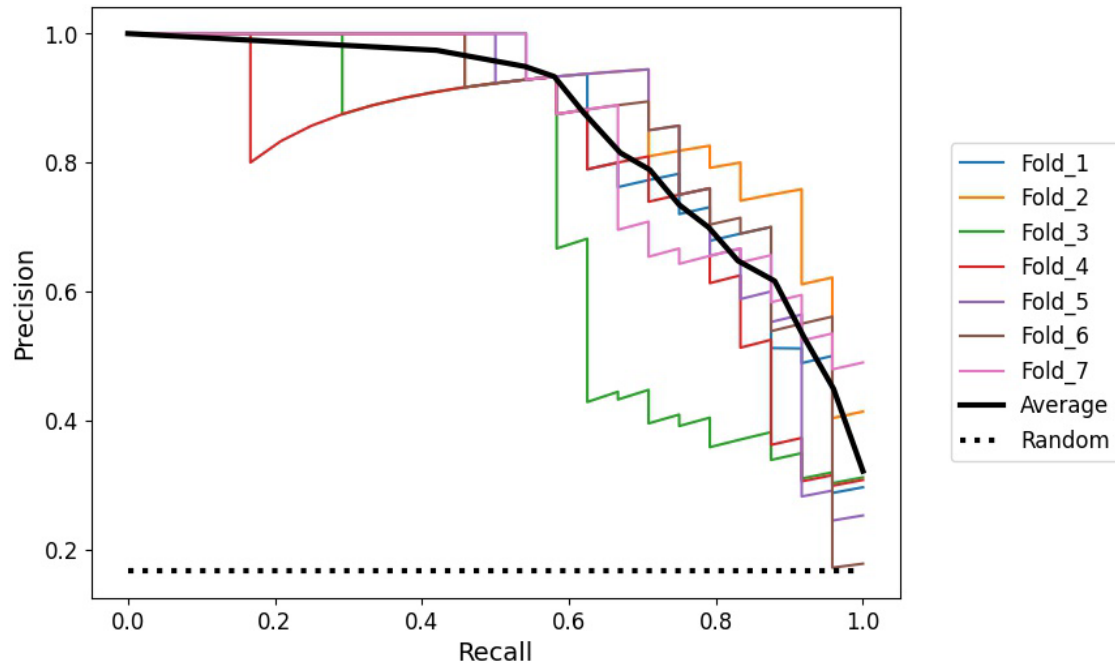
86 In addition, we evaluated the classifier by the determination of the specific image area that was  
87 important for class prediction. We employed the gradient-weighted class activation mapping  
88 technique (Grad-CAM) [24] to present the most significant regions for screening CAC in order to  
89 verify that the classifier indeed concentrated on the calcification areas when it predicted CAC. Figure  
90 2. presents Grad-maps which highlight the important regions in the image for predicting both “CAC”  
91 and “clean” - thus providing "visual explanations" to the predictions. These maps show that the  
92 classifier indeed focused in the calcification areas of the CAC images. It can be noticed that the  
93 region of the calcification signs is the most significant for the CAC prediction. Other Grad-CAM  
94 images can be found in supplementary Figures S3 and S4.

95 **Table 1:** Performance of predicting CAC from panoramic images.

	recall	precision	F1	specificity	accuracy
Average*	0.82	0.71	0.76	0.93	0.91
Std	0.11	0.05	0.08	0.01	0.03

96 \*7-folds CV

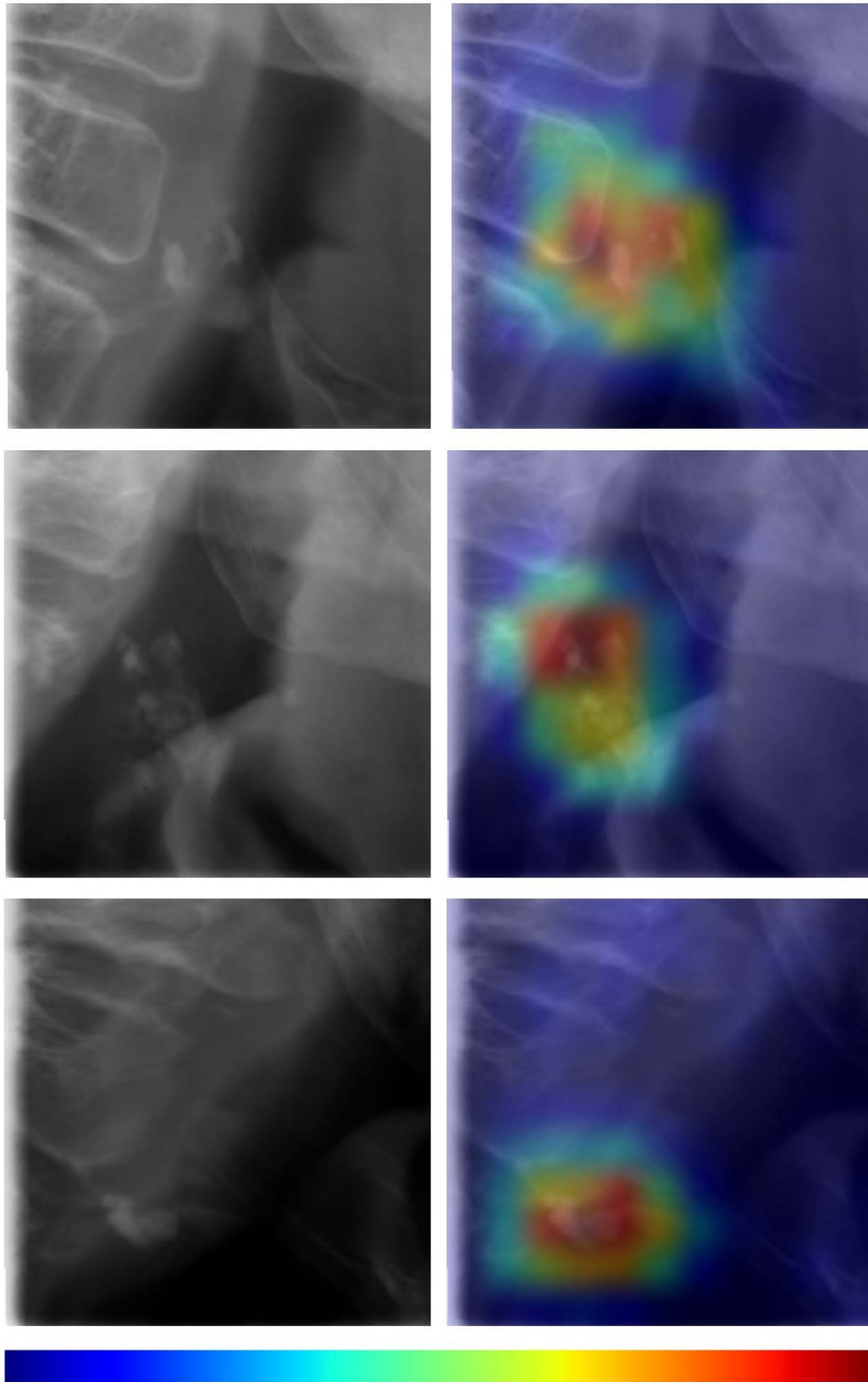
97



98

99 Figure 1: Recall-Precision (RP) curves of all the cross-validation folds (each fold is shown here in a

100 different curve) Random classifier is depicted in dashed line.



102

103 Figure 2. gradient-weighted class activation mapping (Grad-CAM) of a correct prediction of CAC and  
104 “clean” classes. The colors indicate the region that has the greatest impact on the CAC prediction.  
105 The color range is presented below (ranging from red, representing the regions with the greatest  
106 impact on the CAC prediction, to blue, representing the regions with the lowest impact). It can be  
107 noticed that the classifier indeed focused in the region of the calcification signs. Other Grad-CAM of  
108 CAC and clean predications can be found in the supporting information Figures S3 and S4.

109

110 We used the  $p_1$  (recall - probability of predicting the actual calcified corners out of the true calcified  
111 corners and  $p_2$  (specificity - probability of predicting “clean” out of the true clean corners) that were  
112 calculated *per corner* (0.82, 0.93 respectively) as in Table 1 in order to calculate the performances  
113 *per patient*.

114 Assuming that 1/3 of the CAC patients are MM and the other two thirds are CM [25], and that the  
115 ratio of CAC vs. clean is 1:5, the *probabilities* of predicting X or C on the three types of patients with  
116 the actual  $p_1$  and  $p_2$  from the performance on a single side is presented in Table 2. Suppose the  
117 dataset consists of 144 patients as follows: 8 MM, 16 CM and 120 CC we would get the confusion  
118 matrix presented in Table 2. We therefore can use this table to calculate the performance per  
119 patient (see the methods section).

120 **Table 2: The probabilities and quantities of prediction “CAC” or “Clean” on three types of patients**  
121 **based on the performance of a single side. The cells in the table consist of the probabilities and the**  
122 **quantities are presented in parentheses in italic.**

	MM	CM	CC
Clean	0.03 <i>(0.26)</i>	0.17 <i>(2.68)</i>	0.86 <i>(103.69)</i>



<b>CAC</b>	0.97 (7.74)	0.83 (13.32)	0.13 (16.21)
------------	----------------	-----------------	-----------------

123 We calculated the table using  $p_1=0.82$  and  $p_2=0.93$  from the single corner prediction.

124 Assuming the dataset consists of 144 patients as follows: 8 MM, 16 CM and 120 CC, the resulting  
125 calculated performance per patients is presented in Table 3. Recall (sensitivity) of 0.88, precision of  
126 0.57 and specificity of 0.86.

127 The increase in the recall is due to higher probability of correctly predicting the “CAC” of the MM  
128 patients compared to the prediction for an individual corner. The decrease in the precision and  
129 specificity is due to the higher probability of mistakenly predicting “CAC” in the CC patients compare  
130 to the prediction for a single corner.

131

132 **Table 3. Summary - performances of per corner and per patient**

	<b>per side</b>	<b>per patient</b>
<b>recall (sensitivity)</b>	0.82	0.88
<b>specificity</b>	0.93	0.86
<b>precision</b>	0.71	0.57

133

## 134 **Discussion**

135 Prediction of stroke is still one of the major challenges in western medicine. Atherosclerosis of the  
136 carotid arteries is an important etiology for ischemic stroke. The main risk factors for atherosclerosis  
137 are hypertension, diabetes, hyperlipidemia, (hyperlipidemia), high cholesterol levels, smoking and  
138 obesity, all of which cause endothelial cell dysfunction. Atherosclerosis tends to calcify over the  
139 years. Therefore, carotid artery calcification is a manifestation of advanced atherosclerosis in the

140 carotid arteries as well as a marker for atherosclerosis in other blood vessels, including coronary  
141 artery disease and peripheral vascular disease in the lower extremities. Early diagnosis of carotid  
142 arteries calcification (atherosclerosis) would prevent stroke by diagnosing, monitoring and treating  
143 carotid arteries stenoses as well as detecting and treating risk.

144 Carotid calcifications can be detected by performing a carotid ultrasound screening, but this is not a  
145 routine procedure, and is usually recommended only when a murmur is detected on auscultation or  
146 upon evidence of lower limb peripheral vascular disease, or in the presence of medical conditions  
147 that increase the risk of stroke. Periodic ultrasound screenings of the carotid arteries could detect  
148 carotid arteries atherosclerosis and calcification before the appearance of clinical manifestation,  
149 however such a policy involves a huge financial burden and is impractical. CT angiography is another  
150 test that detects atherosclerosis and calcification in carotid arteries, it involves the injection of  
151 contrast material and exposure to x-ray ionizing irradiation in addition to significant financial  
152 expenses, which make this test inadequate for screening purposes. From the other end, panoramic  
153 dental X-rays may provide important information on carotid artery calcification [26-29]. They are  
154 performed routinely and the information on possible CAG can be retrieved without additional clinical  
155 test or procedure. .

156 In this work we developed an AI-based algorithm that can efficiently diagnose calcified  
157 atherosclerosis in the carotid arteries, using routine panoramic dental X-rays images. Such diagnosis  
158 once available, should direct the treating physician to refer the patient for further evaluation and  
159 treatment of carotid artery narrowing, risk factors for atherosclerosis in various blood vessels,  
160 including those causing coronary artery disease and peripheral vascular disease of the lower limbs.

161 The first challenge in this study is the absence of a typical constant shape of the calcification signs –  
162 *i.e.* there are general characteristics for CAC that are common to a wide range of shapes and  
163 orientations. Additionally, this region in the panoramic images contains background noise and other  
164 organs/bones, including the hyoid bone and various shapes of the spinal cord. This together with the

165 relatively small number of samples, which complicate the convergence and generalization. One  
166 approach we used to cope with this challenge, was using the TL, that was successfully implemented  
167 in previous medical studies, including AI-based studies that analyzed panoramic radiographs [14-15].

168 We believe that higher number of images would result in better performance.

169 Computer aided screening of calcification in radiological images is not specific only to the current  
170 topic. There are other procedures in which it can be adopted, such as for detecting coronary  
171 calcification in intravascular optical coherence tomography OCT and detecting calcifications in  
172 breast mammograms. Several studies aimed to computationally screen calcifications using AI and  
173 CNN approaches have been published: Li *et al.* used CNN to automate the segmentation and  
174 quantify coronary calcification in intravascular OCT images, reaching a F1 score of 0.96 [30];  
175 Fuhrman *et al.* developed an algorithm based on both CNN Support vector machine (SVM) algorithm  
176 to classify coronary artery calcifications in low dose thoracic CT [31]. Other studies used a variety of  
177 deep neural network approaches based on CT images to predict different pathologies, such as  
178 transcatheter aortic valve replacement [32], chemotherapy response in breast cancer [33],  
179 quantitative assessment of liver trauma [34], and even the evaluation of complications associated  
180 with metastatic spine tumor surgery [35].

181 Panoramic radiographs are a routine part of oral and maxillofacial examinations. The high number  
182 of panoramic X rays performed routinely in dental clinics can provide an important and efficient tool  
183 for the early detection of calcifications. Nevertheless, due the inadequate training and awareness of  
184 dental personnel in detecting pathologies of the neck region, especially carotid artery calcifications,  
185 results in ignoring of vast amounts of available information that have a high potential for diagnosis,  
186 prevention and monitoring of atherosclerotic changes in carotids. We believe that the current study  
187 lays the foundation for a valuable clinical tool to help health professionals for referring patients to  
188 an appropriate specialist. This novel clinical tool, may be used on wide basis in healthcare  
189 organizations, both dental and medical.

190

191 The present study has several limitations. The manual labeling (by a physician) is challenging: CACs  
192 can be confused with other soft tissue calcifications in the same radiologic region, such as the  
193 triticeous cartilage calcification. However, it is not possible to make a conclusive diagnosis without  
194 doppler ultrasonography, which is used as the gold standard for the diagnosis of atherosclerosis [36].  
195 Because of the retrospective design of this present study, doppler ultrasonographic screening could  
196 not be used as a reference. In addition to the aforementioned small population, a possible limitation  
197 may be in the representation of the overall population, mostly due to the relatively high proportions  
198 of the elderly (which are in any case more susceptible to strokes), or the fact that the method of  
199 diagnosing carotid artery calcification relies on expert diagnosis and not on other laboratory  
200 examinations.

201

202 We intend to conduct further research that will compare machine diagnosis to carotid ultrasound  
203 and angio-CT. In addition, the results of the present study need to be confirmed by larger series. The  
204 prevalence of the real CACs in the predicted positives is only 68%. We anticipate that larger sample  
205 would improve this parameter. However, this study has significant strengths: good AI performance,  
206 mostly the high recall (0.82) and the specificity (0.93), a significant benefit is the ability to assess the  
207 algorithms' performance for a patient, rather than just a corner, and, above all, the potential  
208 implication of this study in clinics and healthcare organizations, enabling a non-invasive, efficient  
209 and applicable solution to understanding the potential and benefits of the early detection of carotid  
210 calcification, both on a patient level and throughout healthcare systems.

211

212 In summary, this study shows the potential and feasibility of applying deep learning-based methods  
213 in an actual "real-world" application of automatic screening for CAC in standard panoramic dental X-  
214 rays. Applying this approach may significantly contribute to quality of life of populations and save  
215 many lives.

## 216 **Materials and methods**

### 217 **Study population and ethical approval**

218 This study was approved by the Poriya Medical Center Institutional Review Board (approval # POR-  
219 0008-21) and was performed in accordance with the Declaration of Helsinki, seventh revision (2013).

220 In total, the study included 500 patients who visited the oral and maxillofacial department at the  
221 Poriya Medical Center between 2016 and 2021 and met with the following criteria. This  
222 retrospective research was based on data from the department's archive, all cases were  
223 anonymized. Informed consent was not required by the ethical committee.

224 Inclusion criteria were as follows: (a) patients who were 40 years old and older, and (b) had a  
225 panoramic radiograph encompassing both jaws (upper and lower), the hyoid bone, and the fourth  
226 upper cervical spine vertebrae. Exclusion criteria were as follows: (a) low quality panoramic  
227 radiographs with trimmed corners and/or blurred and spread spinals; (b) treatment with coumadin  
228 (warfarin); (c) diagnosis of hypomagnesemia; and (d) diagnosis of hypercalcemia due to malignancy.

229 The following parameters were elicited anonymously from the patients' medical files: age, sex,  
230 smoking, alcohol and drug abuse, weight, height, physical activities and systemic medical history.

### 231 **Panoramic radiographs**

232 All the panoramic radiographs were performed on a Planmeca ProMax® 3D (Planmeca Oy, Finland).

233 The clinical files and panoramic radiographs were anonymized.

### 234 **Image labeling**

235 The panoramic images were labeled by several physicians, including certified oral and maxillofacial  
236 physicians, using the location, texture, and morphologic features of stained areas in the images, as  
237 defined and described in previous works [18-20]. The images were labeled to two classes:

238 (a) carotid calcification (CAC) - non-homogeneous irregular calcifications located adjacent to C3-C4  
239 intervertebral space. These characteristics differentiate CAC from other calcifications such as  
240 triticeous cartilage calcification (see supplementary figures S1 and S2, depicting various examples of  
241 CACs and triticeous cartilage calcification); and

242 (b) no carotid calcification (including “clean” images with no calcification and calcification from non-  
243 carotid sources such as triticeous cartilage calcification). Both sides (corners), the left carotid artery  
244 and the right carotid artery, were labelled individually (*i.e.* two labels for each panoramic image).

#### 245 **Data Preprocessing**

246 The main location of CACs is adjacent to C3-C4 spinals. We filtered out images with trimmed corners  
247 and/or with low quality corners such as very blurred and spread spinals in the areas of interest. The  
248 final dataset consists of 480 clean and 179 CAC corners.

249 Since the location of the calcifications of the carotid artery is adjacent to the spinal cord, we cut out  
250 each of the lower corners of the panoramic image in 500 X 500 pixels size (depicted in Fig 3). Each  
251 corner was analyzed separately.

252



253

254 Figure 3. The region of interest is located near the C3-C4 spinals. Therefore, we cut out each of the  
255 lower corners of the panoramic image in 500 X 500 pixels size (depicted with light blue rectangles).  
256 This size ensured that the corners encompassed the calcification.

## 257 **Convolutional neural networks (CNN) and Transfer Learning (TL)**

258 We trained CNN using a TL approach based on the pre-trained InceptionResNetV2 architecture [21].  
259 We replaced the original top layer with 1024 and 256 dense layers followed by 20% drop out. We  
260 used cross-entropy loss function (a detailed representation of the model architecture is depicted in  
261 supplementary Table S1).  
262 We carried out two train routines: an initial train of only the top layer followed by a full model train.  
263 We used the Keras and TensorFlow libraries (version 2.6.0) [22]. Next, we use the trained CNN  
264 (without the top layers) to extract features from the images and fed these features into XGBoost  
265 [23] (version 1.5.2) classifier.

## 266 **Algorithm evaluation**

267 Due to the relatively small number of corners, we evaluated the algorithm performance using a 7-  
268 fold cross-validation approach. We created an imbalance in the folds of 1:5 CAC as a reasonable  
269 balance between “real-world” occurrence rates and the requirement to emphasize carotid  
270 calcification. In each fold we split the data into three sets: (a) test set – with 24 CAC corners and 120  
271 clean ones, (b) validation set – with 24 CAC corners and 120 clean ones, and (c) training set - with  
272 131 CAC corners and 240 clean ones.

273 The performance of the network model after concatenation can be evaluated by determining  
274 statistical values (recall, specificity, precision, and accuracy) and the F1-score. The recall, known also  
275 as “sensitivity” reflects the positive proportion of correct recognition  $\left(\frac{True\ positive}{True\ positive + False\ negative}\right)$ ,  
276 the specificity reflects the negative proportion of correct predictions  $\left(\frac{True\ negative}{True\ negative + False\ positive}\right)$ ,

277 the precision is the fraction of the correct predictions among the retrieved instances

278  $\left(\frac{\text{True positive}}{\text{True positive} + \text{False positive}}\right)$ . F1-score is an evaluation index which takes both precision and recall

279 into account  $\left(2 * \frac{\text{precision} * \text{recall}}{\text{precision} + \text{recall}}\right)$ .

280 **Calculation of prediction per patient (two sides) from prediction of the individual sides**

281 This analysis was meant to calculate the algorithms’ performances focusing on patients rather than  
 282 on individual corners. The statistical calculations are based on the corner classification algorithms  
 283 and their performances. As described before, each panoramic image (of a specific patients) has two  
 284 corners. Therefore, there are three types of patients: (a) a patient with two clean corners (Clean-  
 285 Clean – CC); or (b) a patient with one clean corner and one carotid calcified corner and one clean  
 286 corner (Calcified-Clean – MC); or (c) two carotid calcified corners (MM).

287 We used the performance on a single corner (presented in Table 1) to calculate:

- 288 •  $p_1$  = probability of predicting the actual calcified corners out of the true calcified corners  
 289 (also known as the recall).
- 290 •  $1-p_1$  = probability of mistakenly predicting clean corners out of the of true calcified corners.
- 291 •  $p_2$  = probability of predicting “clean” out of the true clean corners (also known as the  
 292 specificity).
- 293 •  $1-p_2$  = probability of predicting “calcified” out of the true clean corners.

294 These probabilities enable calculating the probabilities of each of the following scenarios related to  
 295 the aforementioned three patient types (See Table 1).

296 **Table 1: Probability calculations of the three patient types**

<i>Actual</i>	MM	CM	CC
<i>Prediction</i>			
Clean	(i) $(1-p_1)^2$	(iii) $p_2(1-p_1)$	(v) $p_2^2$



<b>CAC</b>	<i>(ii)</i> $1-(1-p_1)^2$	<i>(iv)</i> $p_2(p_1-1) + 1$	<i>(vi)</i> $1- p_2^2$
------------	---------------------------	------------------------------	------------------------

297

298 *(i)* The probability of predicting a MM patient (with both corners calcified) as “clean” is the  
299 probability of mistakenly predict “clean” on both sides of the MM patient.

300 *(ii)* The probability of predicting a MM patient (with both corners calcified) as “CAC” (with at least  
301 one calcified corner) is the complementary probability 1-the probability calculated in (a).

302 *(iii)* The probability of predicting a CM patient (with one clean corner and one calcified corner) as  
303 “clean” is the multiplication of the specificity (actual clean) by the complementary of the recall.

304 *(iv)* The probability of predicting a CM patient as “CAC” is the complementary probability: 1-the  
305 probability in (c).  $1-p_2(1-p_1) = 1-p_2+p_1p_2 = p_2(p_1-1) + 1$ .

306 *(v)* The probability of predicting a CC patient (with two clean corners) as “clean”, is the multiplication  
307 of  $p_2$  (specificity) of one corner by the specificity of the other corner.

308 *(vi)* The probability of predicting a CC patient (with two clean corners) as “CAC”, is the  
309 complementary probability 1-the probability calculated in (e).

### **Acknowledgements**

We would like to thank Dr. Millie Kaplan Ben-Ari for her significant contribution to the research and to the manuscript.

### **References**

1. Brott TG, Halperin JL, Abbara S, Bacharach JM, Barr JD, Bush RL et al. Guideline on the management of patients with extracranial carotid and vertebral artery disease. J Am Coll Cardiol. 2011;57:516-94.
2. Virani SS, Alonso A, Benjamin EJ, Bittencourt MS, Callaway CW, Carson AP, et al. American heart association council on epidemiology and prevention statistics committee and stroke statistics subcommittee. Heart disease and stroke statistics-2020 update: a report from the American Heart Association. Circulation. 2020 Mar 3;141(9):e139-596.
3. GBD. Lifetime Risk of Stroke Collaborators. Global, regional, and country-specific lifetime risks of stroke, 1990 and 2016. 2016. New England Journal of Medicine. 2018;379:2429-37.

4. Bengtsson VW, Persson GR, Berglund J, Renvert S. Carotid calcifications in panoramic radiographs are associated with future stroke or ischemic heart diseases: a long-term follow-up study. *Clinical Oral Investigations*. 2019;23:1171-9. <https://doi.org/10.1007/s00784-018-2533-8>
5. Akkemik O, Kazaz H, Tamsel S, Dündar N, Sahinalp S, Ellidokuz H. A 5 years follow-up for ischemic cardiac outcomes in patients with carotid artery calcification on panoramic radiographs confirmed by doppler ultrasonography in Turkish population. *Dento maxillo facial radiology*. 2020;49. <https://doi.org/10.1259/dmfr.20190440>
6. Bengtsson VW, Persson GR, Renvert S. Assessment of carotid calcifications on panoramic radiographs in relation to other used methods and relationship to periodontitis and stroke: a literature review. *Acta odontologica scandinavica*. 2014;72:401-12.
7. Schroder AG, de Araujo CM, Guariza-Filho O, Flores-Mir C, de Luca Canto G, Porporatti AL. Diagnostic accuracy of panoramic radiography in the detection of calcified carotid artery atheroma: a meta-analysis. *Clinical Oral Investigations*. 2019;23:2021-40.
8. LeCun Y, Bengio Y, Hinton G. Deep learning. *Nature*. 2015;521: 436-44.
9. Tajbakhsh N, Shin JY, Gurudu SR, Hurst RT, Kendall CB, Gotway MB, Liang J. Convolutional neural networks for medical image analysis: Full training or fine tuning?. *IEEE transactions on medical imaging*. 2016;35:1299-312.
10. Shin HC, Roth HR, Gao M, Lu L, Xu Z, Nogues I, Yao J, Mollura D, Summers RM. Deep convolutional neural networks for computer-aided detection: CNN architectures, dataset characteristics and transfer learning. *IEEE transactions on medical imaging*. 2016;35:1285-98.
11. Karpathy, A., 2016. CS231n Course Notes: Transfer Learning.
12. Abdelmaksoud, IR, Shalaby A, Mahmoud A, Elmogy M, Aboelfetouh A, El-Ghar, A, El-Melegy M et al. Precise Identification of Prostate Cancer from DWI Using Transfer Learning. *Sensors*, 21(11), p.3664
13. Cha KH, Hadjiiski LM, Chan HP, Samala RK, Cohan RH, Caoili EM, et al. Bladder cancer treatment response assessment using deep learning in CT with transfer learning. In *Medical Imaging 2017: Computer-Aided Diagnosis 2017*;10134: 14-19. SPIE.
14. Mori M, Ariji Y, Katsumata A, Kawai T, Araki K, Kobayashi K, et al. A deep transfer learning approach for the detection and diagnosis of maxillary sinusitis on panoramic radiographs. *Odontology*. 2021;109:941-8.
15. Lee KS, Jung SK, Ryu JJ, Shin SW, Choi J. Evaluation of transfer learning with deep convolutional neural networks for screening osteoporosis in dental panoramic radiographs. *Journal of clinical medicine*. 2020;9:392.
16. Ankenbrand MJ, Lohr D, Schlötelburg W, Reiter T, Wech T, Schreiber LM. Deep learning-based cardiac cine segmentation: Transfer learning application to 7T ultrahigh-field MRI. *Magnetic Resonance in Medicine*. 2021 Oct;86(4):2179-91.
17. Shaik NS, Cherukuri TK. Transfer learning based novel ensemble classifier for COVID-19 detection from chest CT-scans. *Computers in Biology and Medicine*. 2022 Feb 1;141:105127.
18. Carter LC. Discrimination between calcified triticeous cartilage and calcified carotid atheroma on panoramic radiography. *Oral Surgery, Oral Medicine, Oral Pathology, Oral Radiology, and Endodontology*. 2000;90:108-10. <https://doi.org/10.1067/moe.2000.106297>
19. Garay I, Netto HD, Olate S. Soft tissue calcified in mandibular angle area observed by means of panoramic radiography. *International journal of clinical and experimental medicine*. 2014;7(1):51.
20. Azimi S, Sarlak H, Tofangchiha M. Determining the prevalence of carotid artery calcification and associations with medical history using dental panoramic radiographs. *Dental and Medical Problems*. 2016;53:29-33.

21. Szegedy C, Ioffe S, Vanhoucke V, Alemi AA. Inception-v4, inception-resnet and the impact of residual connections on learning. In Thirty-first AAAI conference on artificial intelligence 2017.
22. Abadi M, Barham P, Chen J, Chen Z, Davis A, Dean J, et al. TensorFlow: A System for Large-Scale Machine Learning. In 12th USENIX symposium on operating systems design and implementation (OSDI 16) 2016 (pp. 265-283).
23. Chen T, Guestrin C. XGBoost: A Scalable Tree Boosting System. In: Proceedings of the 22nd ACM SIGKDD International Conference on Knowledge Discovery and Data Mining [Internet]. New York, NY, USA: ACM; 2016. p. 785–94. (KDD '16). Available from: <http://doi.acm.org/10.1145/2939672.2939785>
24. Selvaraju RR, Cogswell M, Das A, Vedantam R, Parikh D, Batra D. Grad-cam: Visual explanations from deep networks via gradient-based localization. In Proceedings of the IEEE international conference on computer vision 2017 (pp. 618-626).
25. Sisman Y, Ertas ET, Gokce C, Menku A, Ulker M, Akgunlu F. The prevalence of carotid artery calcification on the panoramic radiographs in Cappadocia region population. *European journal of dentistry*. 2007;1:132-8.
26. Kats L, Vered M, Zlotogorski-Hurvitz A, Harpaz I. Atherosclerotic carotid plaques on panoramic imaging: an automatic detection using deep learning with small dataset. *arXiv preprint arXiv:1808.08093*. 2018 Aug 24.
27. Kats L, Vered M, Zlotogorski-Hurvitz A, Harpaz I. Atherosclerotic carotid plaque on panoramic radiographs: neural network detection. *Int J Comput Dent*. 2019 Jan 1;22(2):163-9.
28. Çetin MB, Sezgin Y, Yilmaz MN, Seçgin CK. Assessment of carotid artery calcifications on digital panoramic radiographs and their relationship with periodontal condition and cardiovascular risk factors. *International Dental Journal*. 2021;71:160-6.
29. Carasso S, Porat Ben Amy D, Issawy M, Kusniec F, Ghanim D, Sudarsky D et al. The association between carotid calcium on dental panoramic radiographs and coronary calcium score on chest computerized tomography. *Dentomaxillofacial Radiology*. 2021;50:20200174.
30. Li C, Jia H, Tian J, He C, Lu F, Li K, et al. Comprehensive assessment of coronary calcification in intravascular OCT using a spatial-temporal encoder-decoder network. *IEEE Transactions on Medical Imaging*. 2021.
31. Fuhrman JD, Crosby J, Yip R, Henschke CI, Yankelevitz DF, Giger ML. Detection and classification of coronary artery calcifications in low dose thoracic CT using deep learning. In *Medical Imaging 2019: Computer-Aided Diagnosis 2019*;13:10950:820-5). SPIE.
32. Okuno T, Overtchouk P, Asami M, Tomii D, Stortecky S, Praz F, et al. Deep learning-based prediction of early cerebrovascular events after transcatheter aortic valve replacement. *Scientific reports*. 2021;11:1-10.
33. Qi TH, Hian OH, Kumaran AM, Tan TJ, Cong TR, Su-Xin GL, et al. Multi-center evaluation of artificial intelligent imaging and clinical models for predicting neoadjuvant chemotherapy response in breast cancer. *Breast Cancer Research and Treatment*. 2022;193:121-38.
34. Farzaneh N, Stein EB, Soroushmehr R, Gryak J, Najarian K. A deep learning framework for automated detection and quantitative assessment of liver trauma. *BMC Medical Imaging*. 2022;22:1-3.
35. Massaad E, Bridge CP, Kiapour A, Fourman MS, Duvall JB, Connolly ID, et al. Evaluating frailty, mortality, and complications associated with metastatic spine tumor surgery using machine learning-derived body composition analysis. *Journal of Neurosurgery: Spine*. 2022 ;1(aop):1-1.
36. Khosropanah SH, Shahidi SH, Bronoosh P, Rasekhi A. Evaluation of carotid calcification detected using panoramic radiography and carotid Doppler sonography in patients with and without coronary artery disease. *British Dental Journal*. 2009;207:E8

## Supporting information captions

Table S1 Sequence of layers in the CNN used to predict CAC.

Fig S1. Figures A-D are panoramic CAC Corners. The yellow arrows point toward the plaque location.

Fig S2. Figures E and F are panoramic corners with Triticeous Cartilage calcification. The blue arrows point toward the calcification. Figures G and H are clean normal corners.

Fig S3. MapGrad of calcified corners.

Fig. S4. MapGrad of clean corners.